ASSESSMENT OF CARDIAC DYSFUNCTION

BY ULTRASOUND

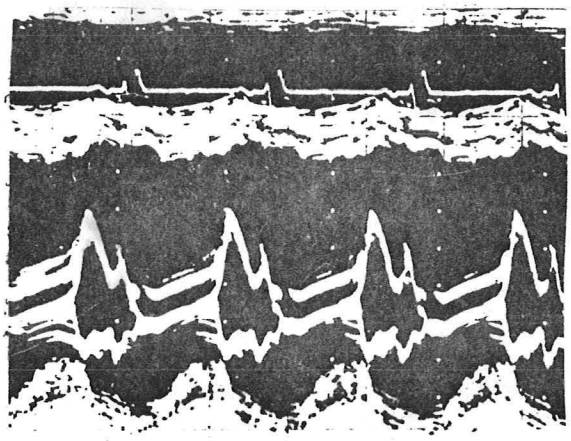

J.V. Nixon, M.D.

Medical Grand Rounds
Southwestern Medical School

Thursday, November 10, 1977

CONTENTS

Reflected ultrasound, although a relatively decent development, has become a well-accepted diagnostic technique in clinical cardiology. It is a safe, noninvasive procedure of minimal inconvenience to the patient. Its principle value lies in the ability to visually display intracardiac structures in considerable detail. Its limitations although few are primarily technical, extending from the physical suitability of the patient to the capability and experience of the examining technician and the interpreting physician.

Even a casual review of the medical literature of the past decade reveals the intense interest of clinical cardiologists in echocardiography. The majority of these publications have been concerned with the association of certain patterns on the echocardiogram with specific cardiovascular disease states. Of greater importance to the clinician has been the trend in the last two or three years to examine the ability of the echocardiogram to directly assess and quantitate cardiac dysfunction. It is this latter concept that I would like to review today. I have selected a few examples of disease states in which attempts have been made using ultrasound to evaluate the severity of the pathophysiology

PHYSICAL PRINCIPLES

The utilization of reflected ultrasound for the assessment of cardiac dysfunction requires a certain basic knowledge of the physical principles involved in the technique. High frequency sound waves of between 1.5 and 5 million cycles per second (megaherz) are pulsed from a focus transducer at a rate of 1000 impulses per second. The beam of sound waves are transmitted through several media including skin, subcutaneous tissue, fat, blood and muscle. Reflection of ultrasonic waves occurs when they encounter an interface between two media of different acoustic impedence. The reflected waveform is then sensed by the amplifying part of the transducer and may be displayed visually in several different ways. All visual displays represent the distance between the transducer and each reflecting interface, based on the principle that sound reflected from more distant objects takes longer to return to the transducer.

The various methods of display of the reflected waveforms include an amplitude or A mode, a brightness or B mode and a motion or M mode. The latter is the conventional display of a diagnostic echocardiogram, when the transducer is placed in the third or fourth left intercostal space on the anterior chest wall (Figure 1).

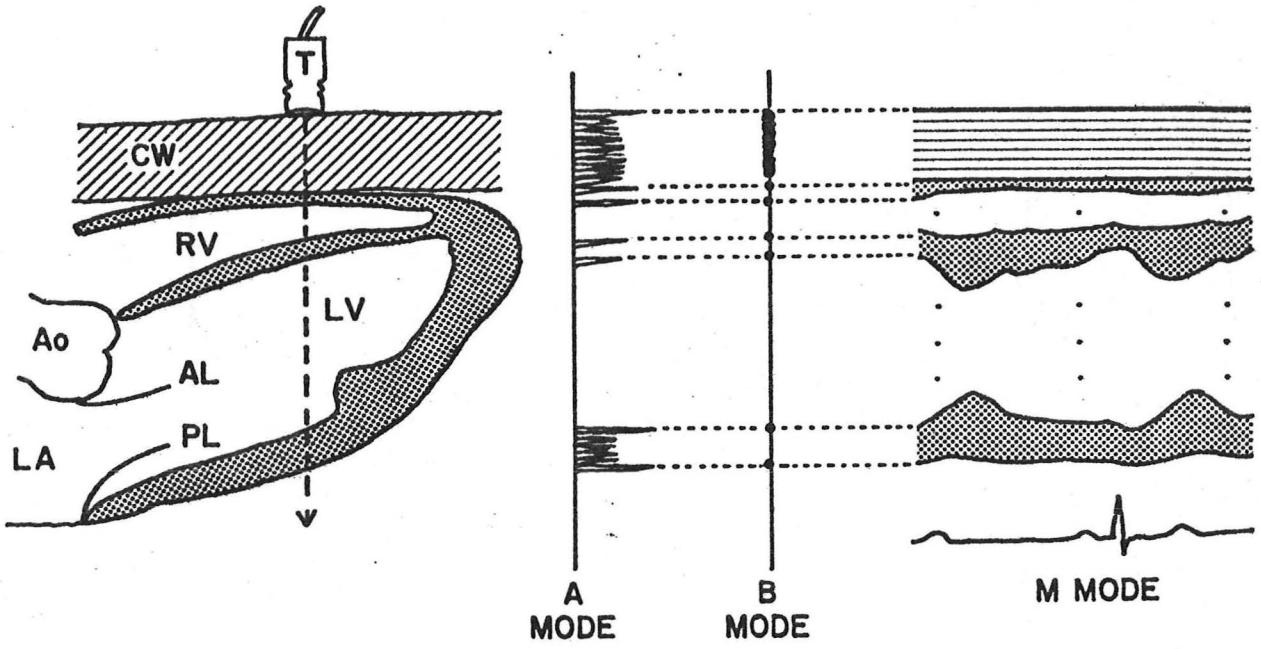

Figure 1: Different methods of ultrasonic display. The transducer (T) is placed on the anterior chest wall (CW) with the broken line indicating the direction of the ultrasound. Corresponding displays of amplitude (A) mode, brightness (B) mode and motion (M) mode are shown, the latter with the concurrent electrocardiogram. RV=right ventricle; LV=left ventricle; Ao-aortic root; LA=left atrium; AL=anterior mitral leaflet; PL=posterior mitral leaflet.

The M-mode recording is a unidimensional, icepick display of reflected echoes within the beam of the transducer. As such, only vertical measurements may be accurately related to distance and the horizontal axis of time is governed by the speed of sweep of the oscilloscope or, in the case of permanent records, of the recording paper. It is important to note that this method of recording does not reflect spatial orientation, a problem which has been recently overcome by the development of cross-sectional or two-dimensional echocardiographic techniques which I will refer to later. Nevertheless, the standard M-mode recording, in addition to identifying patterns of motion of heart walls and valves is very useful in measuring distances, velocities of structural motion and dimensions of cardiac chambers. The concurrent recording of the electrocardiogram permits the identification of motion of the heart walls and valves at various phases of the cardiac cycle.

MITRAL STENOSIS

Mitral stenosis was the first pathological abnormality to be identified by echocardiography (1). Figure 2 illustrates a typical normal echocardiogram and Figure 3 a typical tracing of a patient with severe mitral stenosis.

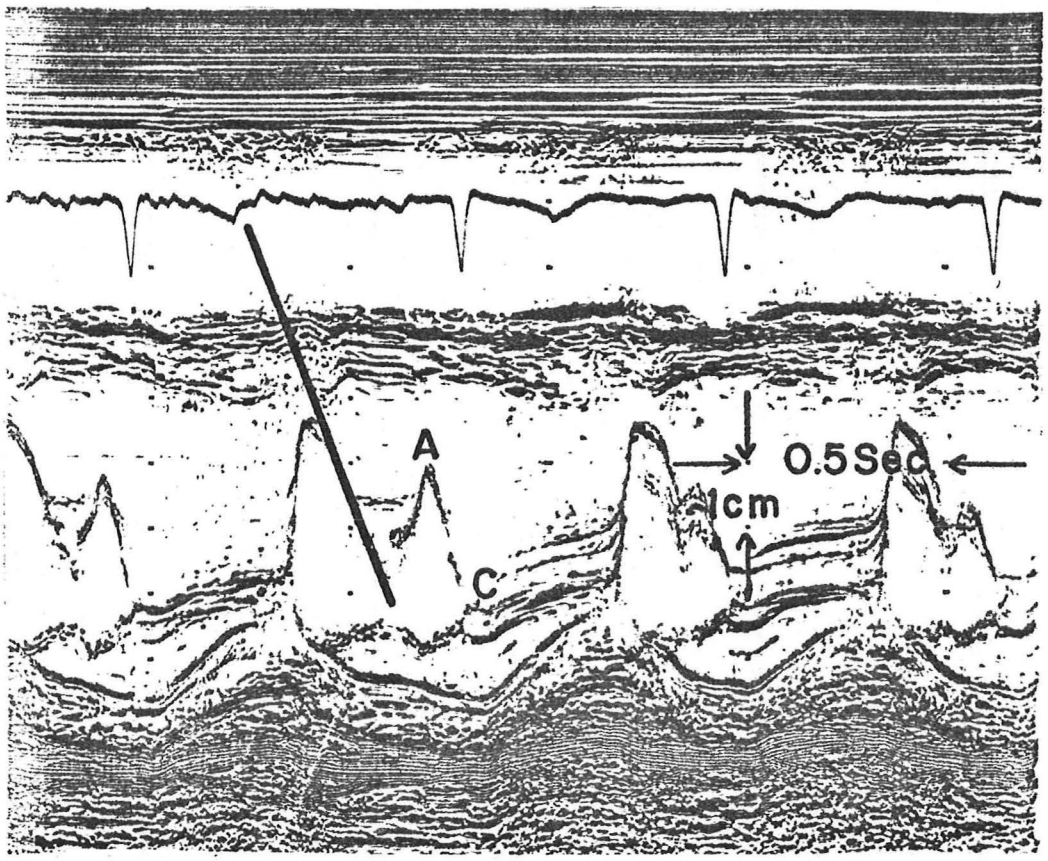

Figure 2: A normal echocardiogram of the mitral valve showing both leaflets. The heavy line represents the early diastolic closing velocity or E to F slope. Letters A and C annote points of change of leaflet motion.

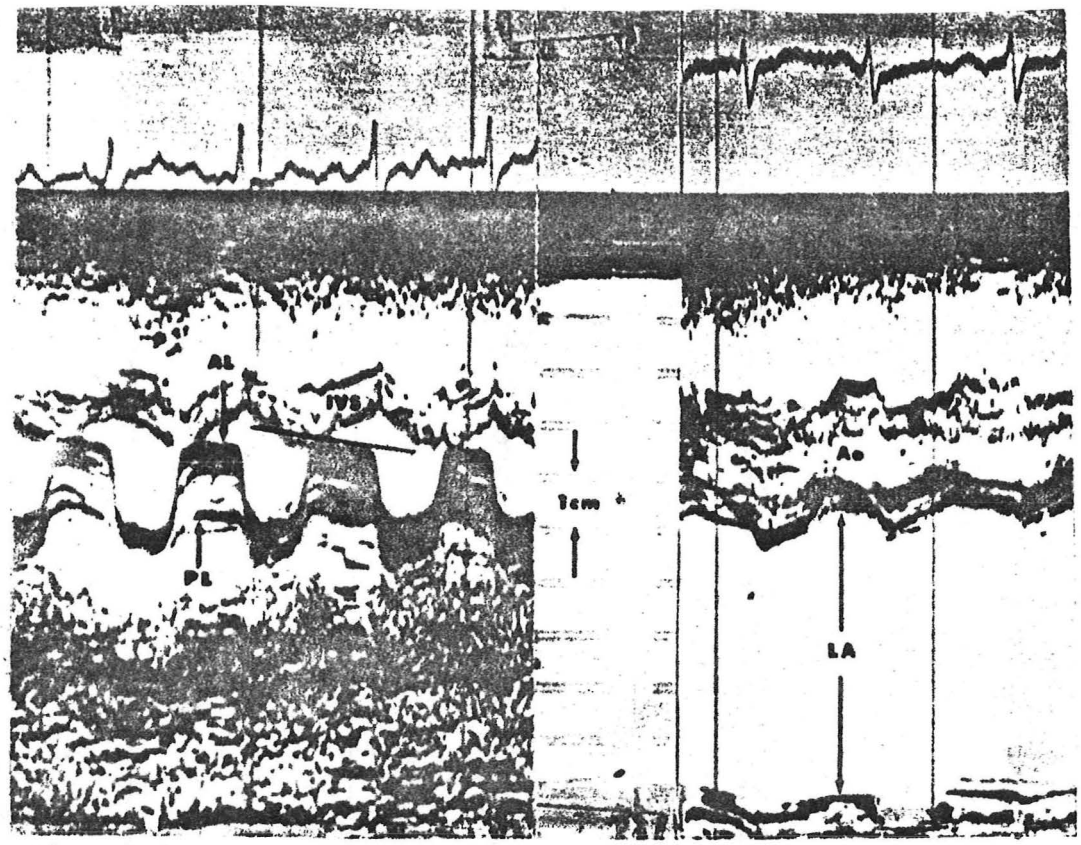

Figure 3: The mitral valve and left atrium in severe mitral stenosis. AL=anterior mitral leaflet, PL=posterior mitral leaflet, IVS=interventricular septum, Ao=aorta, LA=left atrium

The characteristic findings in mitral stenosis are (1) a reduction in the normally rapid early diastolic closing velocity of the anterior mitral leaflet (E to F slope), (2) an increased number of echoes from the mitral leaflets, (3) decreased amplitude of leaflet motion, (4) loss of the A wave, (5) a dilated left atrium, and (6) paradoxical or anterior motion of the posterior mitral leaflet. Several authors have pointed out that all of these features are not necessarily present in every patient with mitral stenosis (2,3).

Since Edler's original observations, there have been many attempts to use the diastolic closing velocity of the anterior mitral leaflet as an estimate of the severity of mitral stenosis. Table 1 lists these studies, comparing the range of echocardiographically estimated mitral valve velocities to the range of mitral valve area calculated by the Gorlin formula at subsequent catheterization (4-9). I have also listed the linear correlation coefficients for the respective studies, all of which reach statistical significiance but show variable material correlation. Similar attempts to correlate the E-F slope with the surgeon's estimate of the severity of the stenosis also showed inconsistent material correlation (5-7, 10-13).

TABLE 1

SUMMARY OF PUBLISHED STUDIES COMPARING
ECHOCARDIOGRAPHICALLY ESTIMATED MITRAL VALVE VELOCITIES
WITH ANGIOGRAPHICALLY ESTIMATED MITRAL VALVE AREAS

Authors	No. of Patients	<15mm/sec		15-25mm/sec		26-35mm/sec		>35mm/sec		R
		No.	Range	No.	Range	No.	Range	No.	Range	
1. Segal et.al.(5)	75	10	0.5-1.0	12	0.5-1.0	19	0.5-2.2	34	0.8-3.0	0.83*
2. Winters et.al.(6)	36	18	0.3-1.6	11	0.4-1.3	4	1.0-2.5	3	1.5-3.2	0.57*
3. Gustafson (7)	25	8	0.8-2.2	14	1.0-2.5	3	1.5-3.5	-	-	0.62
4. Wharton et.al.(8)	24	3	0.5-0.6	8	0.5-1.1	4	1.0-2.5	9	0.8-3.2	0.85*
5. Cope et.al.(9)	61	36	0.5-2.3	16	0.8-2.5	6	1.0-3.5	3	1.8-3.2	0.51

Velocity (mm/sec) refers to mitral valve diastolic closing velocity; range refers to calculated mitral valve area. R = correlation coefficient

*These values were estimated from the figures in the published reports.

Furthermore, a diminished E to F slope is not a finding that is exclusive to mitral stenosis. It has been described in association with left atrial myxoma, left ventricular hypertrophy due to aortic stenosis, both nonobstructive and obstructive forms of asymmetrical septal hypertrophy, right ventricular pressure overload states, and altered left ventricular compliance (14-20).

It is not surprising, then, that attention has been directed elsewhere on the echocardiogram in patients with mitral stenosis. In 1969, it was reported that the left atrial internal dimension on the M-mode tracing correlated well with the maximum left atrial angiographic dimension (21). More recently, Strunk et.al. have shown that, during ventricular diastole, the motion of the posterior aortic wall accurately reflects the left atrial volume curve (22). Figure 4 from their paper illustrates sequential plots of posterior aortic wall motion and left atrial angiographic area during a complete cardiac cycle in two of their patients.

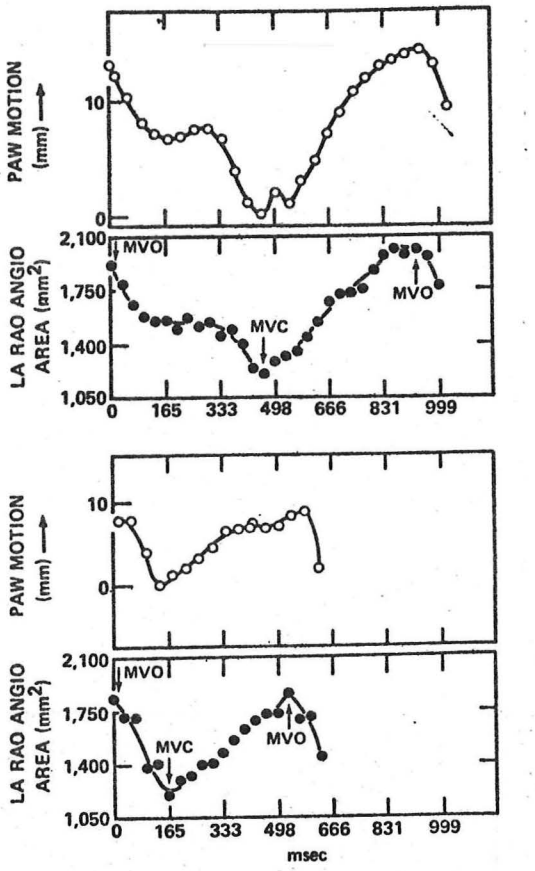

Figure 4: Plots of the posterior aortic root wall (PAW) motion and the left atrial angiographic area in the right anterior oblique view (LA RAO ANGIO) versus time from two patients who had echocardiograms performed simultaneously with angiograms. MVO=Mitral valve opening; MVC=Mitral valve closure (22).

Schematically in Figure 5, they were able to describe posterior aortic wall motion during ventricular diastole reflecting the various phases of left atrial emptying. Their diagram shows the initial rapid phase, the relatively inactive conduit phase and the atrial systolic phase.

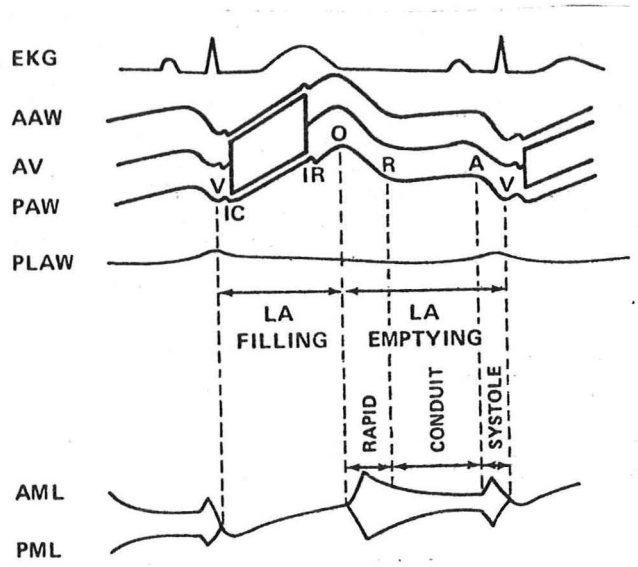

Figure 5: Schematic representation of posterior aortic wall (PAW) motion relative to mitral valve motion. AAW-anterior aortic wall; AV=aortic valve; PLAW=posterior left atrial wall; AML=anterior mitral leaflet; PML=posterior mitral leaflet; V=onset of ventricular systole; IC=isovolumic contraction; IR=isovolumic relaxation; O=onset of left atrial rapid emptying phase; R=onset of left atrial conduit phase; A=onset of left atrial systole (22).

Subsequently, the same group have attempted to estimate the severity of mitral stenosis by the same means (23). Schematic representation of the posterior aortic wall motion of a typical patient is shown in Figure 6.

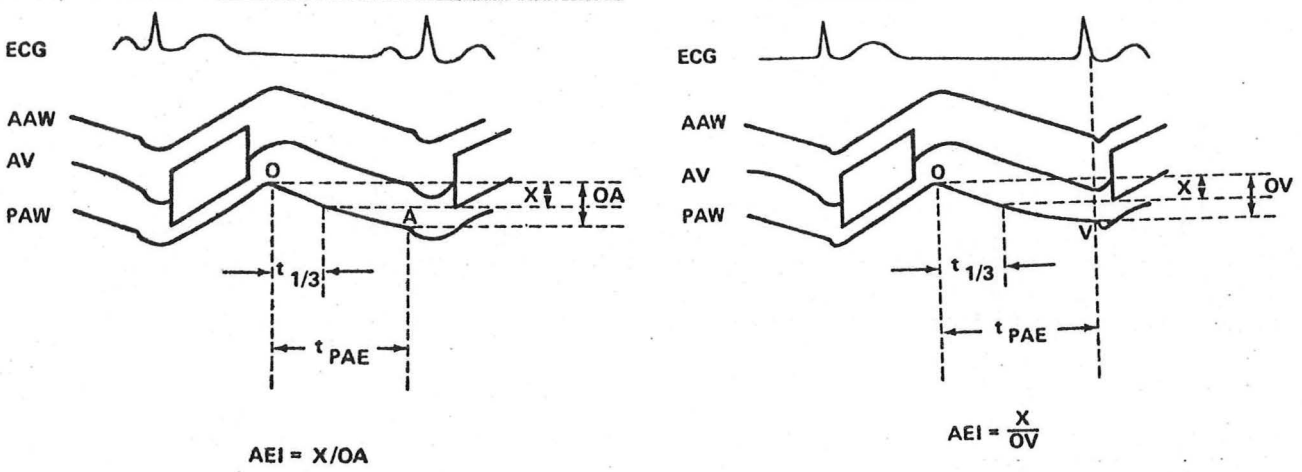

Figure 6: Calculation of the left atrial emptying index (AEI) from the posterior aortic wall (PAW) echo. Time of passive atrial emptying (t_{PAE}) occurs between points O and A. X represents the amplitude of change in PAW motion during the first third of passive atrial emptying; OA represents the amplitude of change during the whole of passive atrial emptying. In a patient with atrial fibrillation, as simulated by the diagram on the right passive atrial emptying is measured to the onset of ventricular systole (V). Other abbreviations as in Figure 5 (23).

They expressed the amplitude change in the first third proportional to the amplitude change during the whole of ventricular diastole as a left atrial emptying index. Figure 7 shows that a linear correlation coefficient

of 0.86 was obtained with a standard error of estimate of 0.1 sq cm/m^2 (This SEE was not quoted and has been estimated from the figure).

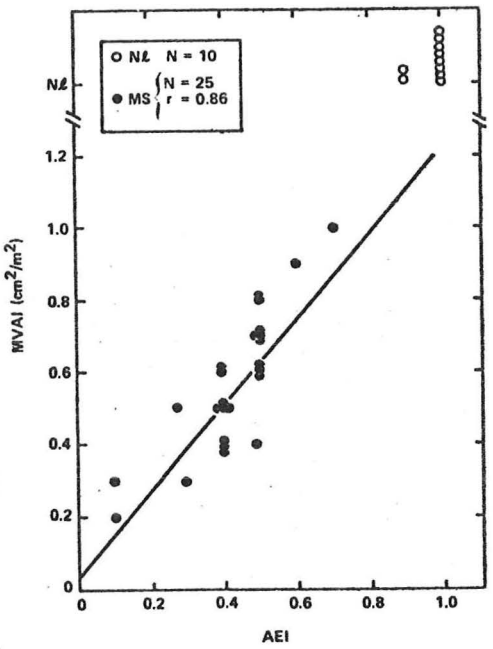

Figure 7: Plots of the angiographically estimated mitral valve area index (MVAI) versus the echocardiographically estimated left atrial emptying index (AEI) in 25 patients with mitral stenosis (MS) (23).

Also, a substantial increase in the left atrial emptying index was found after the valvular obstruction was relieved by surgical porcine heterograph replacement. The importance of this finding lies in the difficulty of clearly identifying a porcine heterograft by ultrasound, and thus assessing prosthetic valve dysfunction.

These studies were performed on patients with pure mitral stenosis. Similar studies in our laboratory on patients with mitral regurgitation and/or associated aortic valvular disease have correlated with the angiographically determined mitral valve area, with correlation coefficients of 0.88 in patients without and 0.97 in patients with mitral regurgitation (24).

The introduction of real-time, two-dimensional echocardiography has provided a noninvasive method of directly visualizing the mitral valve in cross-section (25,26). Figure 8 shows a typical two-dimensional display of a normal and a stenosed mitral valve (27). Direct planimetry of the mitral valve area in two recently published studies of patients with mitral stenosis were compared with values calculated by the Gorlin formula at catheterization, and linear correlation coefficients of 0.92 and 0.95 were obtained (27,28).

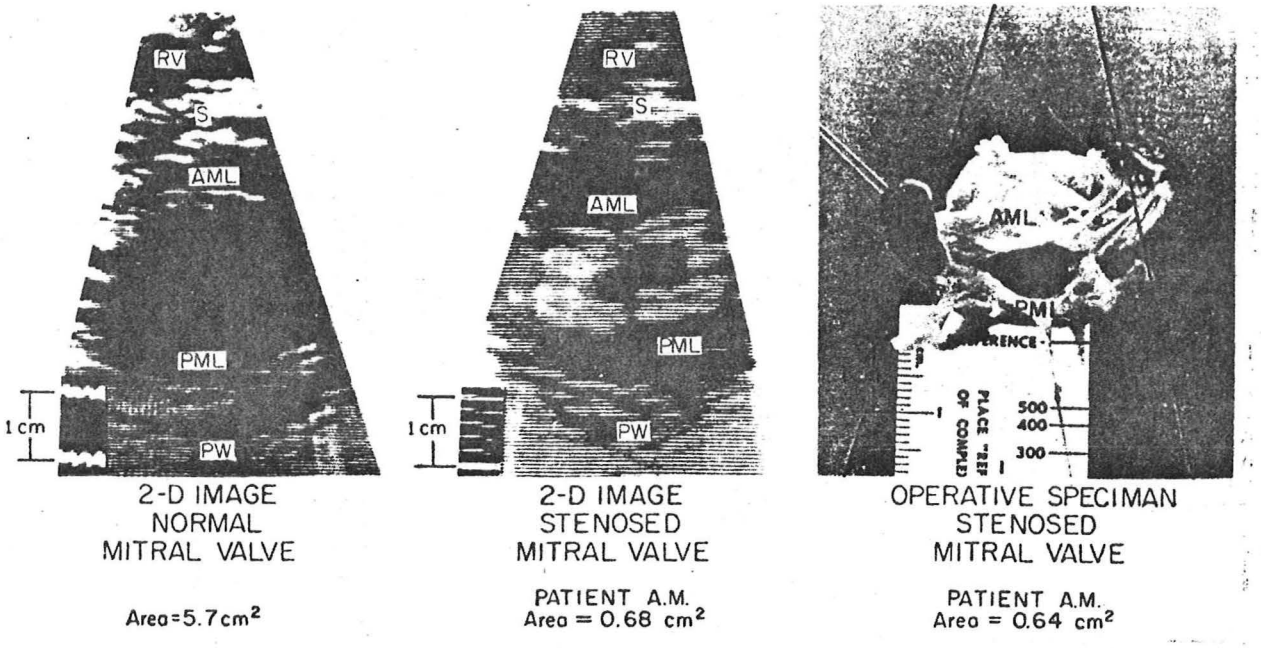

Figure 8: Two-dimensional images of normal and stenosed mitral valves in early diastole with the morphological specimen of the stenosed valve shown on the right. Planimetered areas are given beneath each image. RV=right ventricle; S=septum; AML=anterior mitral leaflet; PML=posterior mitral leaflet; PW=papillary muscle (27).

Thus it is possible to estimate the degree of severity of mitral stenosis by M-mode echocardiography. While real-time, two-dimensional imaging is obviously the method of choice, the prohibitive cost of this equipment currently limits its general use in clinical cardiology.

1. Edler I: Ultrasound cardiogram in mitral valve disease. Acta Clinica Scandinavia, 111:230, 1956.

2. Duchak, JM, Jr., Chang S, Feigenbaum H: The posterior mitral valve echo and the echocardiographic diagnosis of mitral stenosis. Am J Cardiol, 29:260, 1972.

3. Levisman JA, Abbasi AS, Pearce ML: Posterior mitral leaflet motion in mitral stenosis. Circulation, 51:511, 1975.

4. Gorlin R, Gorlin SG: Hydraulic formula for calculation of the stenotic mitral valve, other cardiac valves and central circulatory shunts. Am Heart J, 41:1, 1951.

5. Segal B, Likoff W, Kingsly B: Echocardiography. Clinical application in mitral stenosis. JAMA, 195:99, 1966.

6. Winters WL, Riccetto A, Gimenez J, McDonough M, Soulen R: Reflected ultrasound as a diagnostic instrument in study of mitral disease, Br Heart J, 29:188, 1967.

7. Gustafson A: The correlation between ultrasound cardiography, hemodynamics and surgical findings in mitral stenosis. Am J Cardiol, 19:32, 1967.

8. Wharton CFP, Lopez-Bescos L: Mitral valve movement: A study using an ultrasound technique. Br Heart J, 32:344, 1970.

9. Cope GD, Kisslo JA, Johnson ML, Behar VS: A reappraisal of the echocardiogram in mitral stenosis. Circulation, 52:664, 1975.

10. Joyner CR, Dyrda I, Barrett JS, Reid JM: Preoperative determination of the functional anatomy of the mitral valve. Circulation 32(suppl. II): II-120, 1965.

11. Edler I: Ultrasound cardiography in mitral valve stenosis. Am J Cardiol, 19:18, 1967.

12. Effert S: Pre-and post-operative evaluation of mitral stenosis by ultrasound. Am J Cardiol, 19:59, 1967.

13. Nanda NC, Gramiak R, Shah M, DeWeese JA: Mitral commisurotomy versus valve replacement: pre-operative evaluation by echocardiography. Circulation, 46:835, 1975.

14. Wolfe SB, Popp RL, Feigenbaum H: Diagnosis of atrial tumors by ultrasound. Circulation 39:615, 1969.

15. Shah PM, Gramiak R, Kramer DH: Ultrasound localization of left ventricular outflow obstruction in hypertrophic obstructive cardiomyopathy. Circulation 40:3, 1969.

16. Shah PM, Gramiak R, Adelman AG, Wigle ED: Role of echocardiography in diagnostic and hemodynamic assessment of hypertrophic subaortic stenosis. Circulation, 44:891, 1974.

17. Shabetai R, Davidson S: Asymmetrical hypertrophic cardiomyopathy simulating mitral stenosis. Circulation, 45:37, 1972.

18. McLaurin LP, Gibson TC, Waider W, Grossman W, Craige E: An appraisal of mitral valve echocardiograms mimicking mitral stenosis in conditions of right ventricular pressure overload. Circulation 48:801, 1973.

19. Quinones MA, Gaasch WH, Waisser E, Alexander JK: Reduction in the rate of diastolic dissent of the mitral valve echogram in patients with altered left ventricular diastolic pressure-volume relations, Circulation, 49:246, 1974.

20. DeMaria AN, Miller RR, Amsterdam EA, Markson W, Mason DT: Mitral valve early diastolic closing velocity in the echocardiogram: Relation to sequential diastolic flow and ventricular compliance. Am J Cardiol, 37:693, 1976.

21. Hirata R, Wolfe SB, Popp RL, Helmen CH, Feigenbaum H: Estimation of left atrial size using ultrasound. Am Heart J, 78:43, 1969.

22. Strunk BL, Fitzgerald JW, Lipton M, Popp RL, Barry WH: The posterior aortic wall echocardiogram: its relationship to left atrial volume change. Circulation, 54:744, 1976.

23. Strunk BL, London EJ, Fitzgerald J, Popp RL, Barry WH: The assessment of mitral stenosis and prosthetic mitral valve obstruction, using the posterior aortic wall echocardiogram. Circulation 55:885, 1977.

24. Leonard PD, Nixon JV: Estimation of mitral valve area in patients with mitral stenosis and associated valvular disease by echocardiography. Unpublished Data.

25. Griffith JM, Henry WL: A sector scanner for real-time two-dimensional echocardiography. Circulation, 59:1147, 1974.

26. Von Ramm DT, Thurston FL: Cardiac imaging using a phased array ultrasound system I. Circulation, 53:258, 1976.

27. Henry WL, Griffith JM, Michaelis LL, McIntosh CL, Morrow AG, Epstein SE: Measurement of mitral valve orifice area in patients with mitral valve disease by real-time, two-dimensional echocardiography. Circulation 51:827, 1975.

28. Nichol PM, Gilbert BW, Kisslo JA: Two dimensional echocardiographic assessment of mitral stenosis. Circulation, 55:120, 1977.

LEFT VENTRICULAR DYSFUNCTION

Measurements of the various estimates of left ventricular performance have been the pursuit of physicians interested in echocardiography for many years. The extrapolation of linear dimensions obtained from a single dimensional M-mode study to represent the volume of a three dimensional chamber has obvious drawbacks. Furthermore, there are no means currently of accurately assessing subtle changes in intracavitary pressure by echocardiography. Nevertheless, alterations in ultrasonic measurements do reflect actual and angiographically determined changes in ventricular dimensions in normal and uniformly diseased left ventricles.

The geometric representation of the normal left ventricle as a prolate ellipse has been used routinely in estimating cineangiographic volumes for many years (29). By assuming that the major axis of the geometric shape is twice the minor axis, the volume can be estimated with reasonable accuracy as the cube of the minor diameter (30). Figure 9 shows the minor diameters of the left ventricle at end-diastole and end-systole.

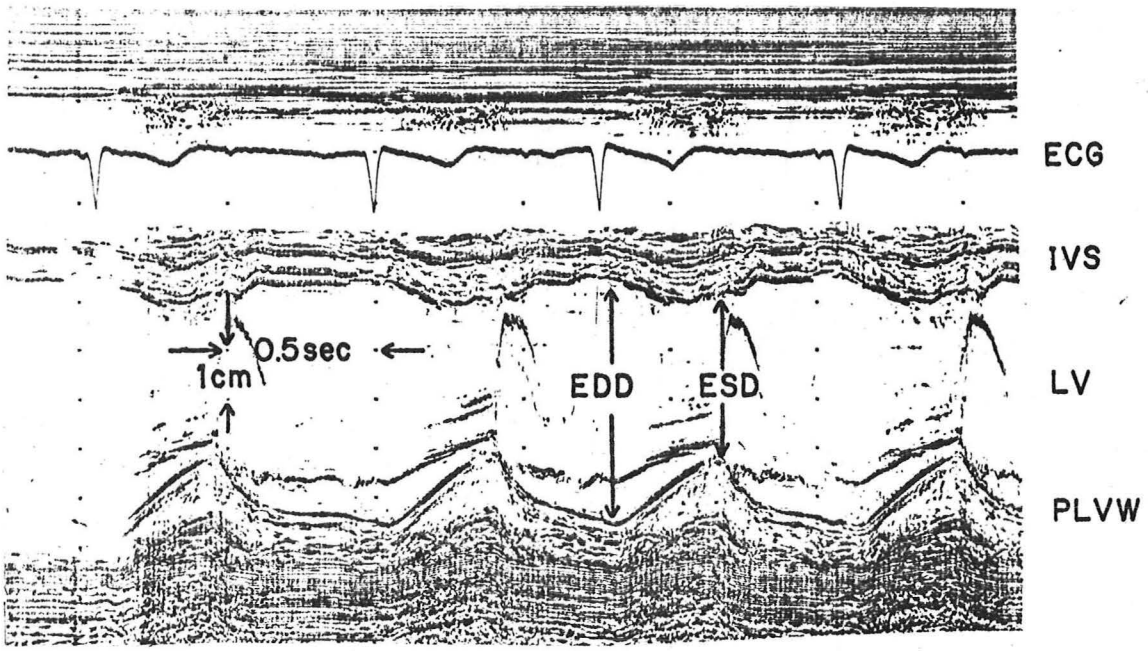

Figure 9: A normal echocardiogram of the left ventricular cavity (LV) showing the points of estimation of the end-diastolic diameter (EDD) and end-systolic diameter (ESD). IVS=interventricular septum; PLVW=posterior left ventricular wall.

In twenty patients with normal left ventricular angiograms, echocardiographic measurements correlated well with angiographic measurements with a standard error of estimate of 8 ml (31) (Figure 10). These findings have been confirmed by several authors and summarized recently by Linhart et.al. (32).

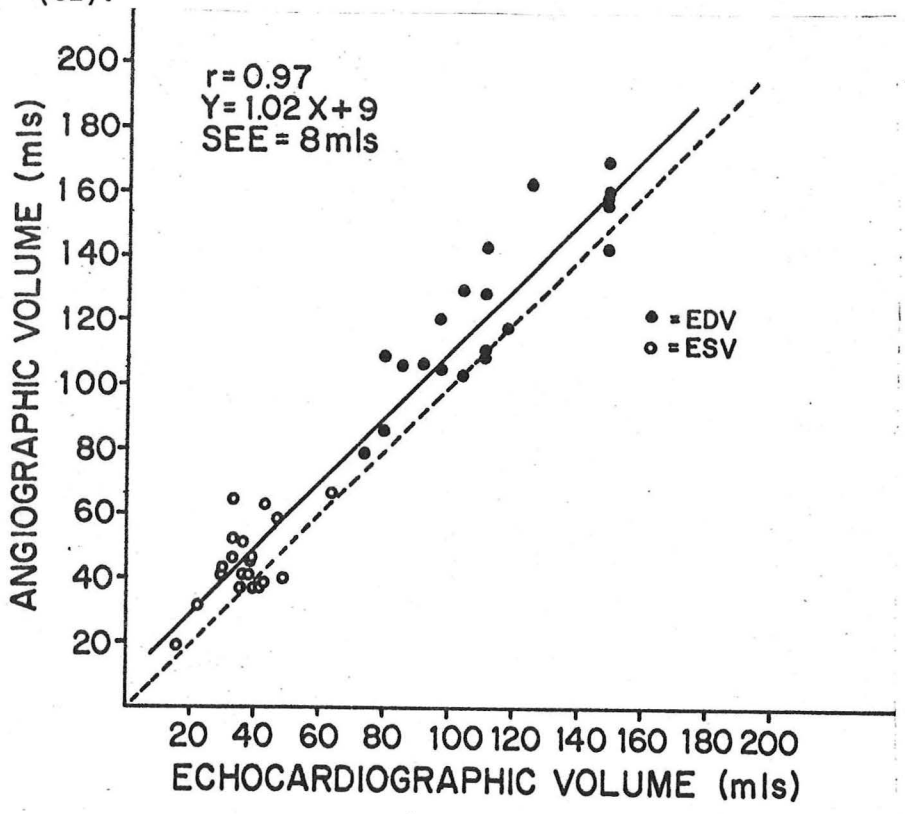

Figure 10: Plots of echocardiographically estimated left ventricular end-diastolic volumes (EDV) and end-systolic volumes (ESV) versus similar cine-angiographically estimated volumes of 20 patients with no evidence of heart disease at cardiac catheterization (31).

The mean velocity of circumferential fiber shortening or the velocity of change of the minor axis circumference during systole has been shown to be an accurate measure of myocardial contractility (33). This can be easily estimated from end-diastolic (EDD) and end-systolic (ESD) dimensions on the echocardiogram, and estimations have been shown to correlate with reasonable accuracy with angiographic measurements (34).

$$\text{Mean VCF} = \frac{\text{EDD-ESD}}{\text{EDD xLVET}}$$

where LVET is the ejection time.

As I have already stated, the echocardiogram is not able to provide direct estimations of left ventricular pressure. However, an abnormal pattern of mitral valve motion, as is shown in Figure 11, has been associated with an elevated left ventricular end-diastolic pressure (35).

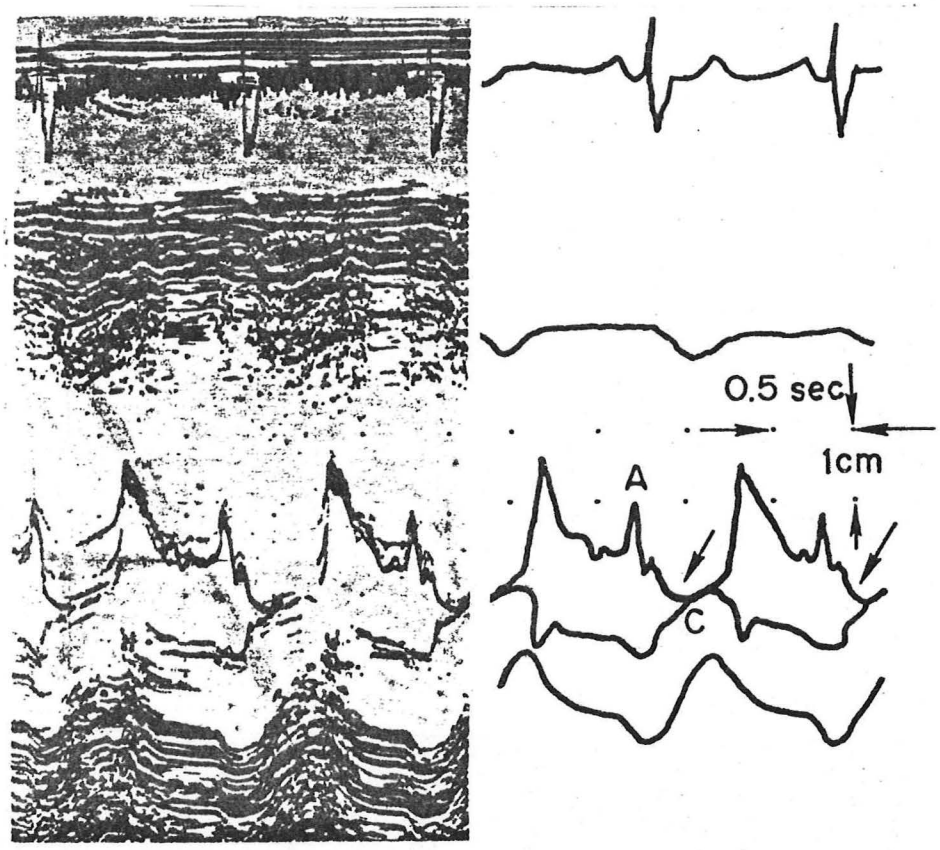

Figure 11: Delayed mitral valve closure (C) indicated by the arrows on the echocardiogram of a patient following an acute myocardial infarction (42).

Because the interval between the A and C points is a function of atrioventricular contraction, this interval was subtracted from the PR interval

on the electrocardiogram. Figure 12 compares the PR-AC interval with the left ventricular end-diastolic pressure in 36 patients, 14 of whom had end-diastolic pressures of greater than 20 mm Hg. All 14 patients had PR-AC intervals of less than 0.06 second (35).

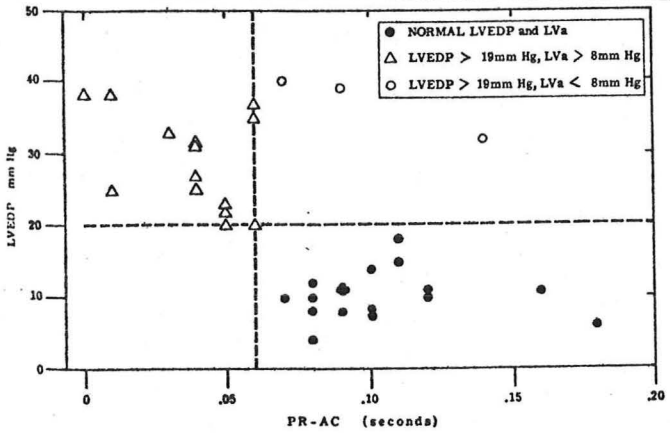

Figure 12: Plots of the PR-AC interval versus the left ventricular end-diastolic pressure (LVEDP). LVa=atrial pressure wave on left ventricular pressure tracing (35).

These estimates of left ventricular function have been used to evaluate patients with valvular heart disease and cardiomyopathies (36-38). The acute effects of low doses of alcohol have been measured by these means (39). Figure 13 shows the reduction in echocardiographic ejection fraction and mean velocity of circumferential fiber shortening for up to ninety minutes after the ingestion of six ounces of whiskey in thirteen normal volunteers.

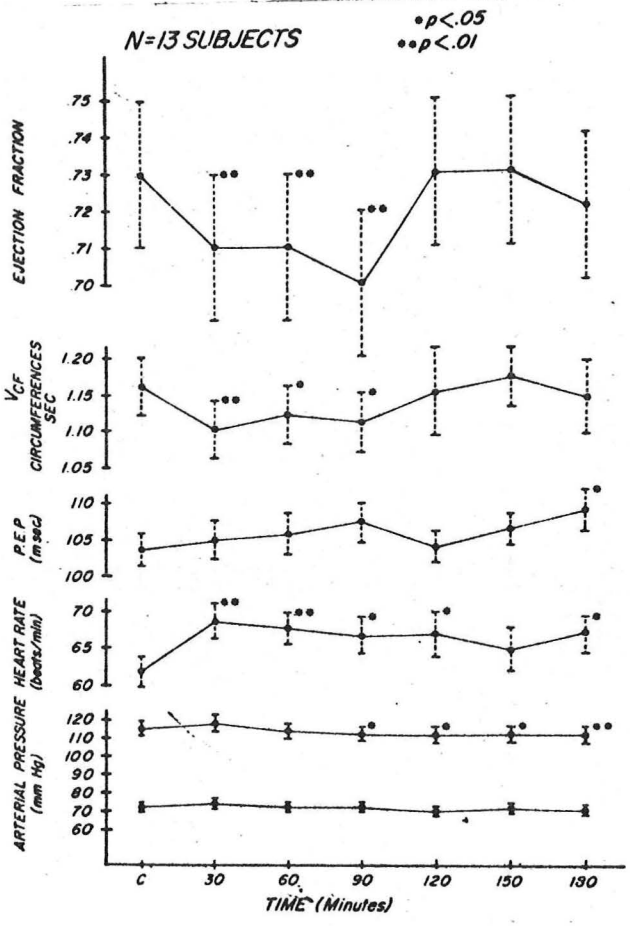

Figure 13: Acute effects of alcohol indigestion on left ventricular ejection fraction, mean velocity of circumferential fiber shortening (Vcf), pre-ejection period (PEP), heart rate and arterial blood pressure in 13 normal volunteers. C= control values (39).

Estimations of ventricular volumes from minor axis dimensions are inaccurate in patients with ischemic heart disease, because of the presence of segmental wall motion abnormalities, (40). Figure 14 demonstrates that while estimations of end-diastolic volumes remain accurate, echocardiographic end-systolic volumes are inconsistent when compared to angiographic measurements (31).

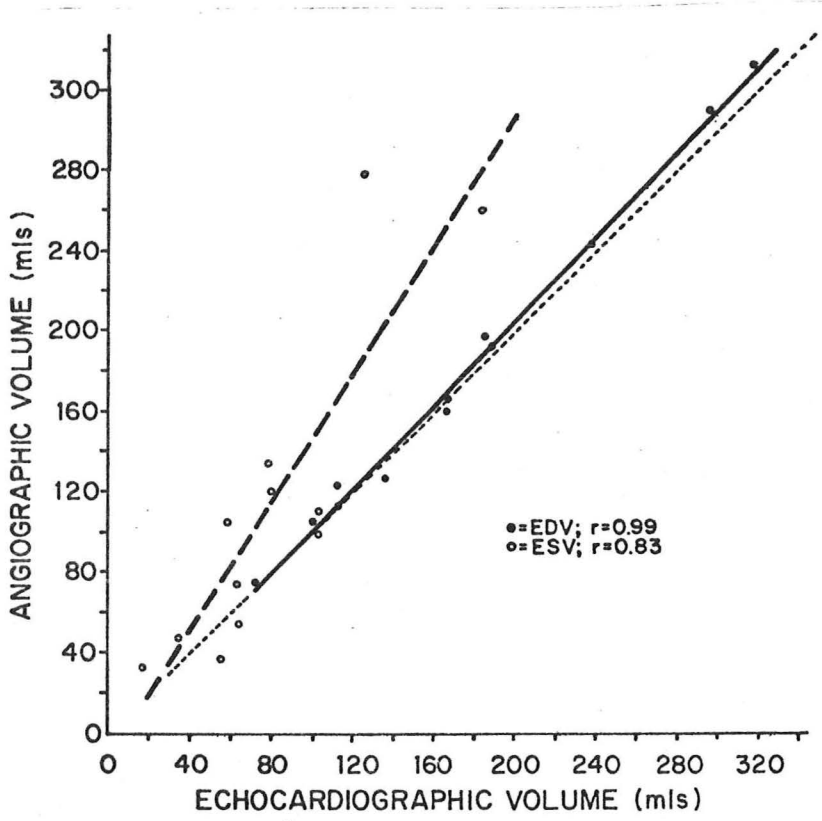

Figure 14: Plots of echocardiographically estimated left ventricular end-diastolic volumes (EDV) and end-systolic volumes (ESV) versus similar cine-angiographically estimated volumes in 13 patients with coronary artery disease and segmental wall motion abnormalities at cardiac catheterization (31).

Left ventricular end-diastolic dimensions have been shown to correlate with the presence of heart failure in patients with acute myocardial infarctions (41,42). Also, an abnormal ratio of the volume estimate (the end-diastolic diameter) to the pressure estimate (the PR-AC time) of the left ventricle has been shown to have prognostic implications. This abnormal ratio has correlated significantly with both inhospital deaths and post-discharge ischemic events following myocardial infarction, identified high risk patients undergoing coronary artery bypass and predicted mortality following left ventricular aneurysmectomy (41-44).

Although a qualitative observation rather than a quantitative estimation, the value of two-dimensional studies in the demonstration of a left ventricular aneurysm should be noted (45,46). Figures 15 and 16 compare the two-dimensional studies of a normal cardiac apex with an apical aneurysm. Both reports confirm that this technique is highly specific.

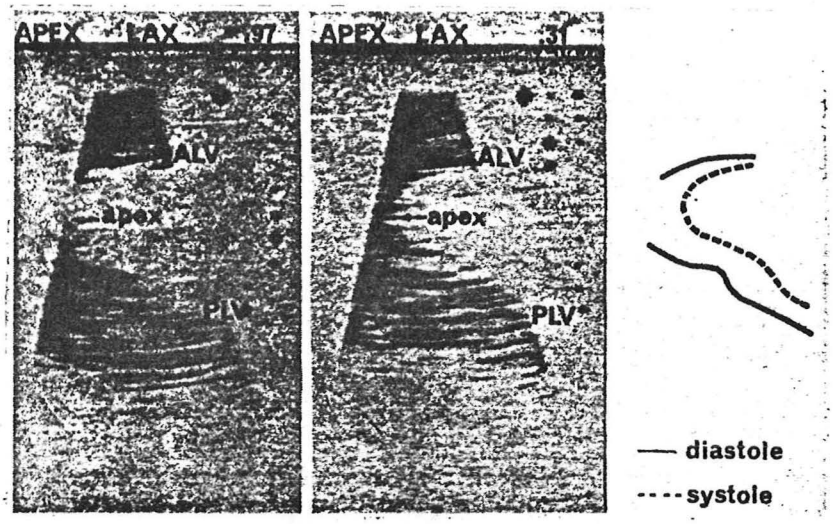

Figure 15: Two-dimensional echocardiogram of the left ventricular apex of a normal subject. ALV=anterior left ventricular wall; PLV=posterior left ventricular wall; LAX=long axis section (45).

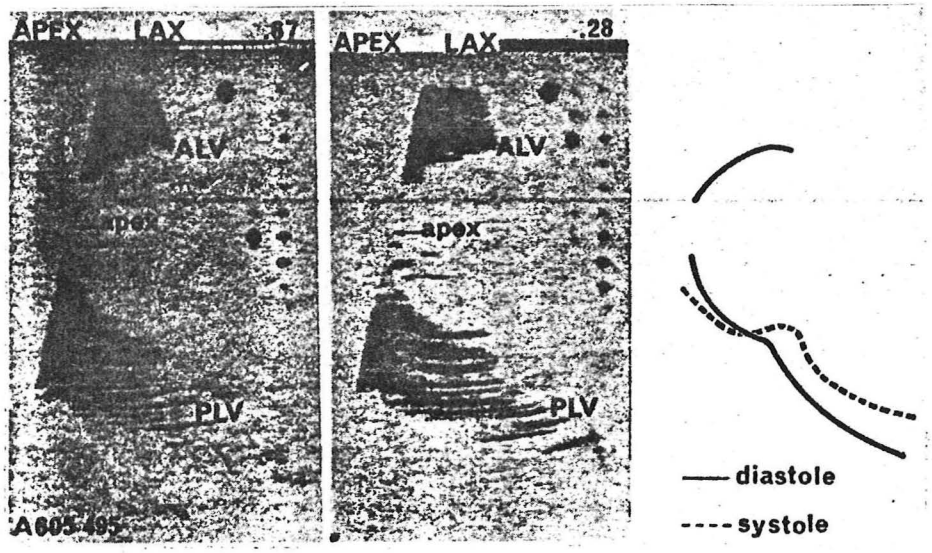

Figure 16: Two-dimensional echocardiogram of the left ventricular apex of a patient with a large apical aneurysm. Abbreviations as in Figure 15 (45).

Estimations of left ventricular mass are also possible by ultrasound. While original determinations were compared to angiographic measurements, a recent study comparing echocardiographic measurements to postmortem weights showed an excellent correlation (47,48) (Figure 17).

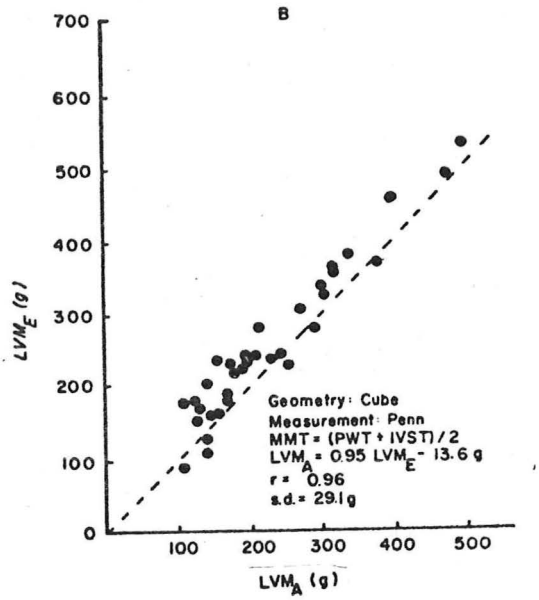

Figure 17: Plots of post-mortem left ventricular weight (LVM_A) versus the echocardiographically estimated left ventricular mass (LVM_E) in 34 patients whose echocardiograms were obtained within 3 months of their death (48).

These methods have been used to investigate the left ventricular mass of patients with arterial hypertension (49). Figure 18 illustrates how we applied this method to confirm the experimental observations that left ventricular mass regresses in thyrotoxic patients treated effectively (50).

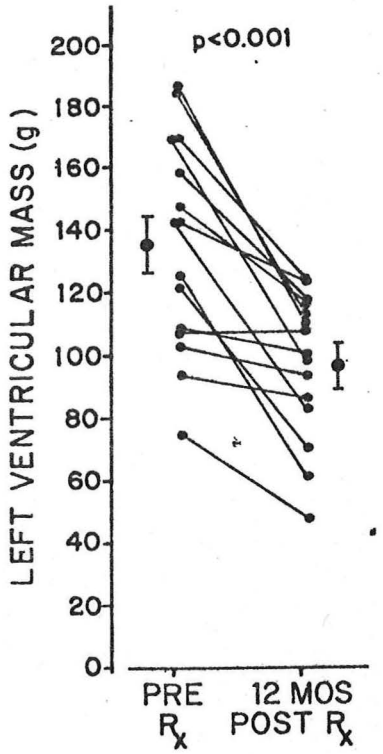

Figure 18: Echocardiographic estimates of left ventricular mass in 15 patients treated effectively for thyrotoxicosis prior to and 12 months after commencement of therapy (Rx) (50).

Thus, ultrasound is a useful means of estimating left ventricular performance in patients with cardiac disease as a single evaluation and in serial studies to determine the progression of disease and the effects of therapy.

29. Dodge HT, Sandler H, Ballels DW: Use of biplane angiography for measurement of left ventricular volume in man. Am Heart J 60:762, 1960.

30. Pombo JF, Troy BL, Russell RO Jr.: Left ventricular volumes and ejection fraction by echocardiography. Circulation, 43:480, 1971.

31. Nixon JV: The utilization of echocardiography in the evaluation of left ventricular function in patients with acute myocardial infarction. Unpublished data.

32. Linhart JW, Mintz GS, Segal BL, Kawai N. Kottler MN: Left ventricular volume measurement by echocardiography: fact or fiction? Am J Cardiol 36:114, 1975.

33. Karliner JS, Gault JH, Eckberg D, Mullins CB, Ross J Jr: Mean velocity of fiber shortening: a simplified measure of left ventricular myocardial contractility. Circulation 44:323, 1971.

34. Ludbrook P, Karliner JS, Peterson K, Leopold G, O'Rourke RA: Comparison of ultrasound and cineangiographic measurements of left ventricular performance in patients with and without wall motion abnormalities. Br Heart J 35:1026, 1973.

35. Konecke LL, Feigenbaum H, Chang S, Corya BC, Fischer JC: Abnormal mitral valve motion in patients with elevated left ventricular diastolic pressures. Circulation 47:989, 1973.

36. McDonald IG: Echocardiographic assessment of left ventricular function in aortic valve disease. Circulation 53:860, 1976.

37. McDonald IG: Echocardiographic assessment of left ventricular function in mitral valve disease. Circulation 53:865, 1976.

38. Abbasi AS: Echocardiography in the differential diagnosis of the large heart. Am J Med 60:677, 1976.

39. Delgado CE, Fortuin NJ, Ross RS: Acute effects of low doses of alcohol on left ventricular function by echocardiography. Circulation 51:535, 1975.

40. Jacobs JJ, Feigenbaum H. Corya BC, Haine CL, Black MJ, Chang S: Echocardiographic detection of left ventricular asynergy. Circulation 46: 42, 1972.

41. Corya BC, Rasmussen S, Knoebel SB, Feigenbaum: Echocardiography in acute myocardial infarction. Am J Cardiol 36:1, 1975.

42. Nixon JV, Kredatus J, Blomqvist CG, Willerson JT: Prognostic value of serial echocardiography in patients with acute myocardial infarction. Clinical Research 25:6, 1977.

43. Corya BC, Rasmussen S, Knoebel SB, Black MJ, Feigenbaum H: Echocardiographic left ventricular function related to coronary bypass mortality. Circulation 52:II-133, 1975.

44. Dillon JC, Feigenbaum H, Weyman AE, Corya BC, Peskoe S, Chang S: M-mode echocardiography in the evaluation of patients for aneurysmectomy. Circulation 53:657, 1976.

45. Weyman AE, Peskoe SM, Williams ES, Dillon JC, Feigenbaum H: Detection of left ventricular aneurysms by cross-sectional echocardiography. Circulation 54:936, 1976.

46. Kisslo JA, Robertson D, Gilbert BW, Von Ramm O, Behar VS: A comparison of real-time, two-dimensional echocardiography and cineangiography in detecting left ventricular asynergy. Circulation 55:134, 1977.

47. Troy BL, Pombo JF, Rackley CE: Measurement of left ventricular wall thickness and mass by echocardiography. Circulation 45:602, 1972.

48. Devereux RB, Reichek N: Echocardiographic determination of left ventricular mass in man: Anatomic validation of the method. Circulation 55:613, 1977.

49. Mehmel HC, Mazzoni S, Krayenbuehl HP: Contractility of the hypertrophied human left ventricle in chronic pressure and volume overload. Am Heart J 90:236, 1975.

50. Nixon JV, Cohen M, Anderson RJ: Changes in left ventricular dimensions and mass in patients treated effectively for thyrotoxicosis. Circulation 56: III-215, 1977.

ASYMMETRIC SEPTAL HYPERTROPHY

Echocardiographic studies have helped considerably to clarify the syndrome formerly known as idiopathic hypertrophic subaortic stenosis or hypertrophic obstructive cardiomyopathy (51,52). Figure 19 illustrates the echocardiographic features of the obstructive form of asymmetric septal hypertrophy, namely, a reduced left ventricular outflow tract, disproportionate hypertrophy of the interventricular septum and systolic anterior motion of the anterior mitral valve leaflet (53).

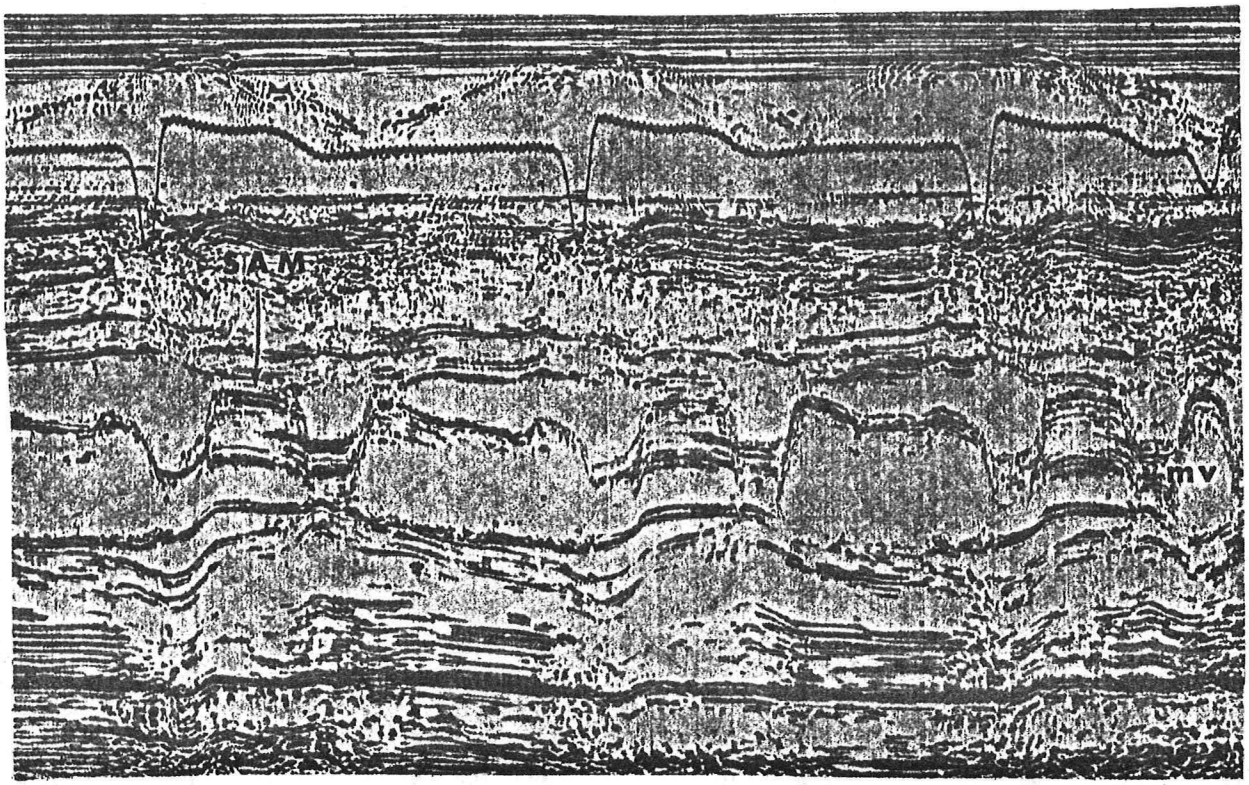

Figure 19: Echocardiogram of a patient with asymmetric septal hypertrophy showing disproportionate hypertrophy of the interventricular septum (IVS) and systolic anterior motion (SAM) of the anterior leaflet of the mitral valve.

Studies by Henry and associates have shown that the characteristic finding in this disease is asymmetric hypertrophy of the interventricular septum compared to the posterior left ventricular wall (54). This finding was present in 100 patients, independent of the presence or absence of left ventricular outflow tract obstruction. Figure 20 compares the findings of patients with 22 normal subjects and 11 patients with fixed left ventricular outflow tract obstruction (55). In every case of asymmetric septal hypertrophy, the ratio of septal to posterior left ventricular wall thickness was greater than 1.3 to 1. In contrast, the same ratio was less than 1.2 to 1 in normal subjects and patients with fixed outflow tract obstruction. Because their studies included patients without the obstructive form of the disease, the same authors concluded that asymmetric septal hypertrophy was the pathognomonic anatomic abnormality.

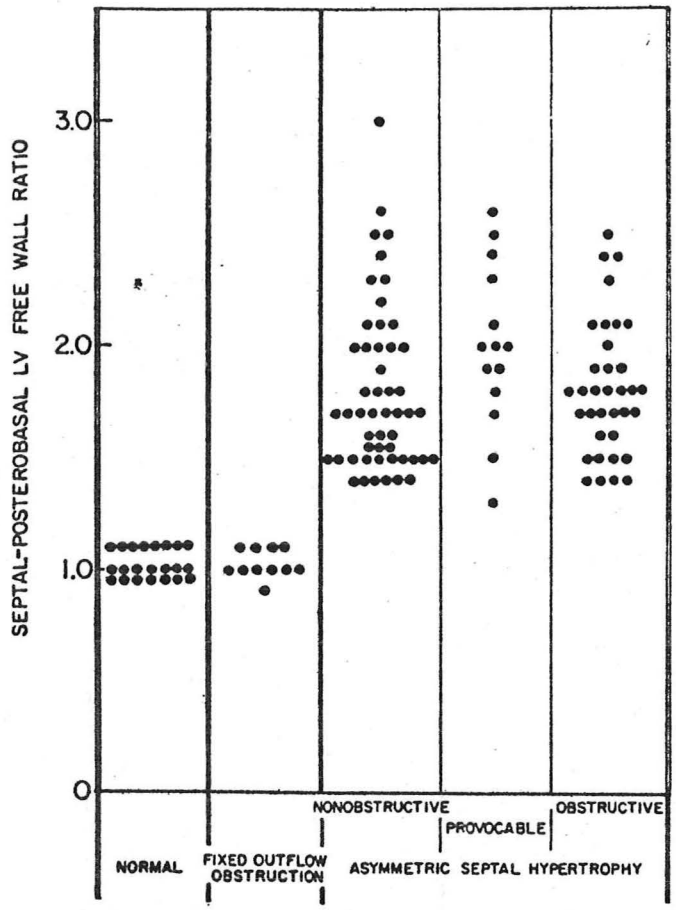

Figure 20: The echocardiographic septal-posterobasal left ventricular free wall ratio in 22 normal subjects, 11 patients with fixed left ventricular outflow tract obstruction and 100 patients with asymmetric septal hypertrophy (55).

Because several previous reports had indicated that this disease was sometimes familial, the same group of investigators obtained echocardiograms from the first-degree relatives of 30 patients with asymmetric septal hypertrophy (56). Figure 21 shows the prevalence of disease in the family members based on their relationship to the respective patient. Twenty-eight patients were found to have at least one affected relative. Parents and siblings were more frequently affected than children. There was no difference in prevalence between males and females. They concluded that most, if not all, patients with asymmetric septal hypertrophy have a genetic defect that is transmitted as an autosomal dominant trait with a high degree of penetrance.

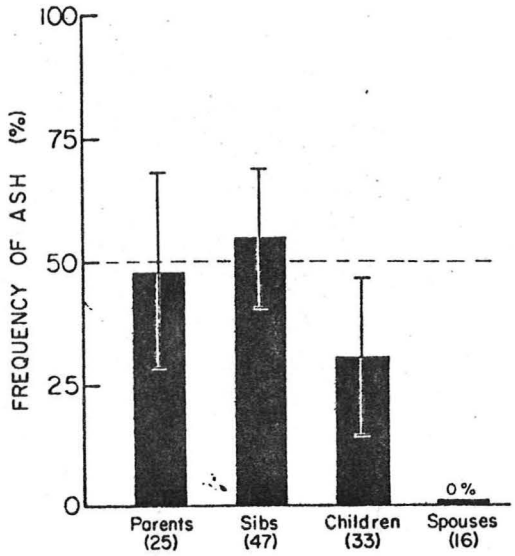

Figure 21: The prevelance of asymmetric septal hypertrophy (ASH) in family members based on their relationship to the respective patient (56).

Finally, Henry and his colleagues directed their attention to patients with the obstructive form of asymmetric septal hypertrophy to examine whether it was possible to estimate the left ventricular outflow tract gradient by echocardiogram (57). Figure 22 shows their method of calculating the obstruction index, where the duration of narrowing of the systolic anterior motion of the anterior mitral leaflet was expressed as a proportion of the average septal-mitral distance.

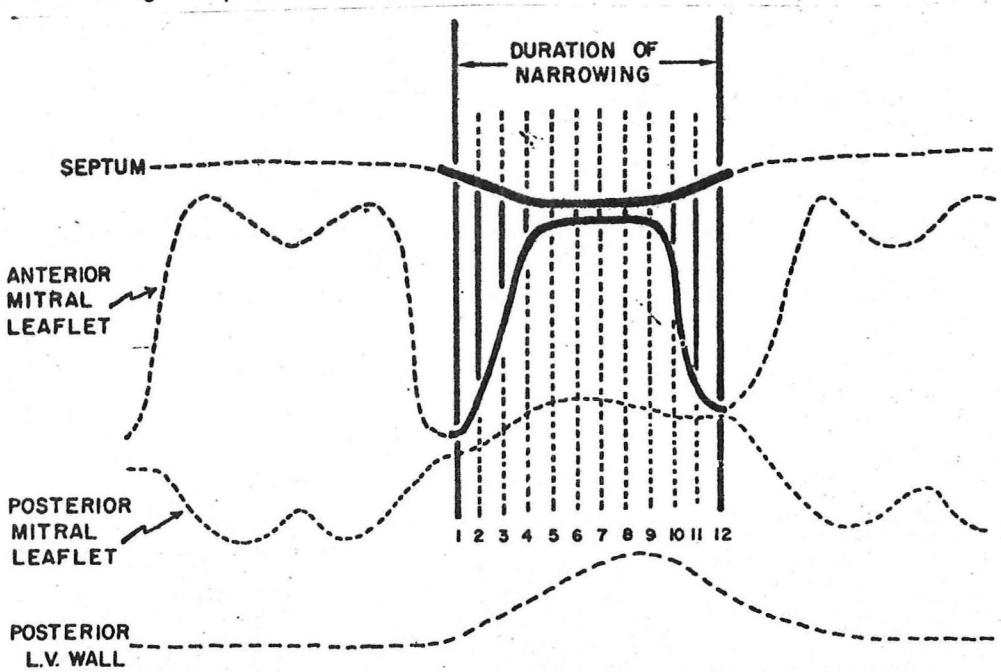

Figure 22: Representation of the method used to calculate the obstruction index in patients with asymmetric septal hypertrophy (57).

Figure 23 illustrates the excellent correlation obtained when the obstruction index was compared to the outflow tract gradient measured during catheterization. They concluded that echocardiography is the preferred technique for the diagnosis of asymmetric septal hypertrophy, because of its ability to identify the disease process in the absence of significantly altered hemodynamics. Furthermore, the echocardiogram is capable of demonstrating the presence or absence of a pressure gradient. When present, the magnitude of the gradient may be calculated by this means.

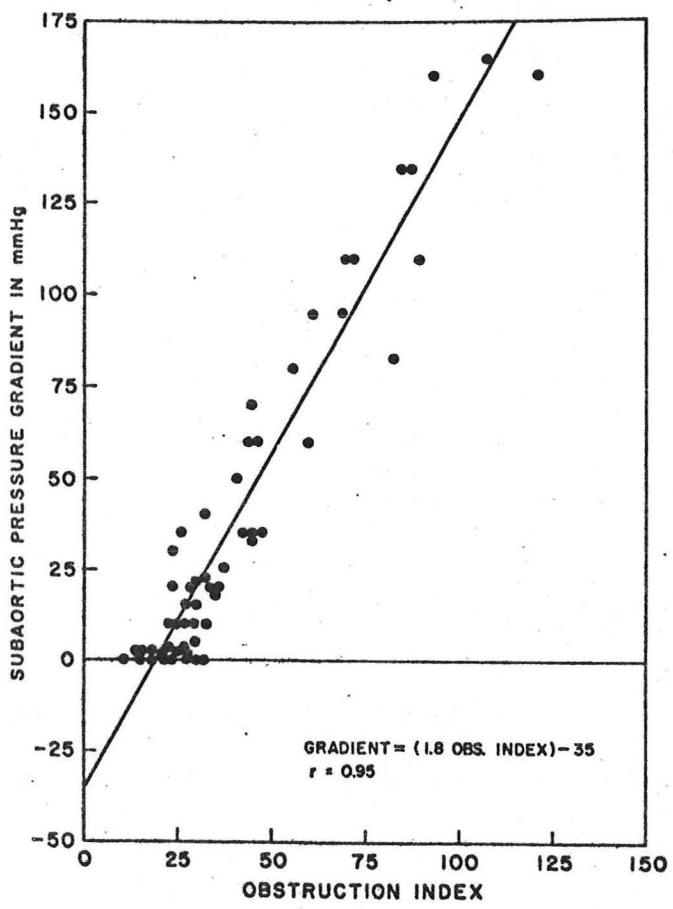

Figure 23: Plots of echocardiographic obstruction index versus simultaneous peak subaortic pressure gradient for 56 individual heart beats in 11 patients (57).

51. Braunwald E, Lambrew CT, Rockoff SD, Ross J Jr, Morrow AG: Idiopathic hypertrophic subaortic stenosis: 1. A description of the disease based on the analysis of 64 patients. Circulation 30:3, 1964.

52. Goodwin JF, Hollman A, Cleland WP, Oakley CM: Obstructive cardiomyopathy simulating aortic stenosis. Br Heart J 22:402, 1960.

53. Rossen RM, Goodman DJ, Ingham RE, Popp RL: Echocardiographic criteria in the diagnosis of idiopathic hypertrophic subaortic stenosis. Circulation 50:747, 1974.

54. Henry WL, Clark CE, Epstein SE: Asymmetric septal hypertrophy: echocardiographic identification of the pathognomonic anatomic abnormality of IHSS. Circulation. 47:225, 1973.

55. Epstein SE, Henry WL, Clark CE, Roberts WC, Maron BJ, Ferrans VJ, Redwood DR, Morrow AG: Asymmetric septal hypertrophy. Ann Intern Med 81:650, 1974.

56. Clark CE, Henry WL, Epstein SE: Familial prevalence and genetic transmission of idiopathic hypertrophic suboartic stenosis. N Engl J Med 289:704, 1973.

57. Henry WL, Clark CE, Glancy DL, Epstein SE: Echocardiographic measurement of the left ventricular outflow gradient in idiopathic hypertrophic subaortic stenosis. N Engl J Med 288:989, 1973.

PERICARDIAL EFFUSION

Echocardiography is considered to be the procedure of choice for evaluating patients suspected of having a pericardial effusion. The demonstration of an echo-free space between the epicardial surface of the posterior left ventricular wall with or without a similar finding between the anterior right ventricular wall and the anterior chest wall indicates the presence of a pericardial effusion (58). These features are illustrated in Figure 24.

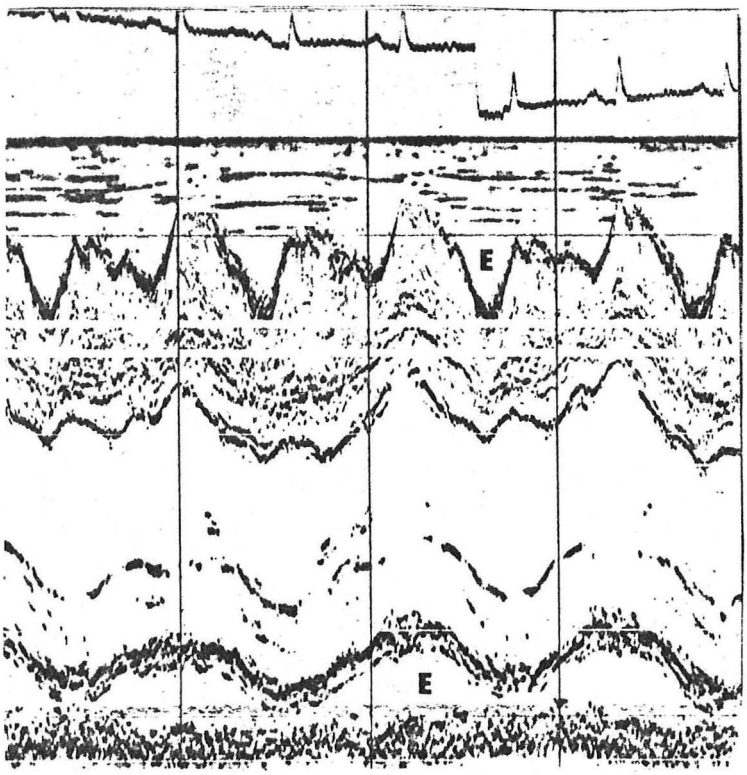

Figure 24: Pericardial effusion with an echo-free space (E) seen both anteriorly and posteriorly.

Since these observations gained general acceptance, some effort has been made to estimate the volume of a pericardial effusion by echocardiography, with only limited success. Horowitz et.al. analyzed the echocardiograms of 39 patients prior to cardiac surgery (59). Several patterns of posterior epicardial and pericardial motion were seen in the presence and absence of pericardial effusion (Figure 25). Patterns A, B and C_1 represented normal variants. Patterns C_2 and D were consistently seen in the presence of small and moderate or large effusions. Pattern E represented a thickened pericardium. They confirmed that pattern D was classical for an effusion.

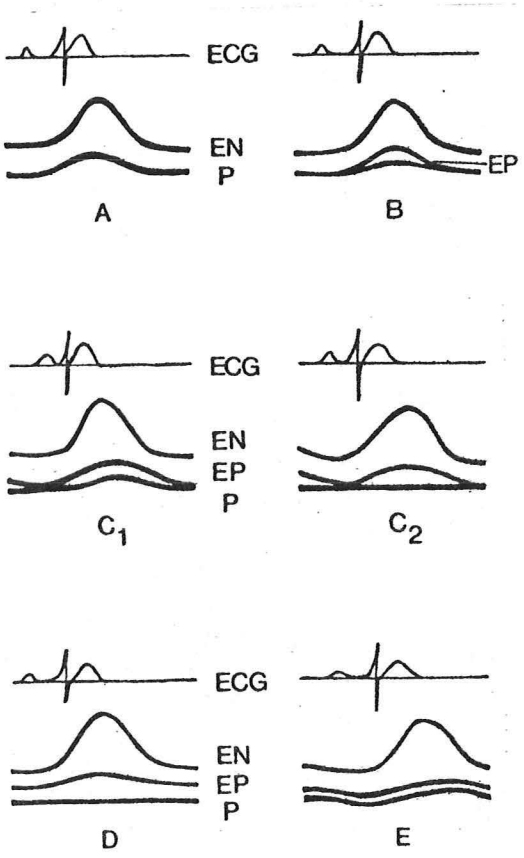

Figure 25: Patterns of posterior epicardial and pericardial movement in the presence and absence of pericardial effusions. Patterns A, B and C_1 were found in patients without effusion. C_2 represents a small effusion. D is the classical pattern. E represents a thickened pericardium (59).

The same authors also attempted to quantitate the size of the pericardial effusion by devising a method of estimating volume similar to the method used for the echocardiographic estimation of left ventricular mass (47). The comparison between the ultrasonic estimations and the actual volumes of 12 patients measured at cardiac surgery are shown in Figure 26A.

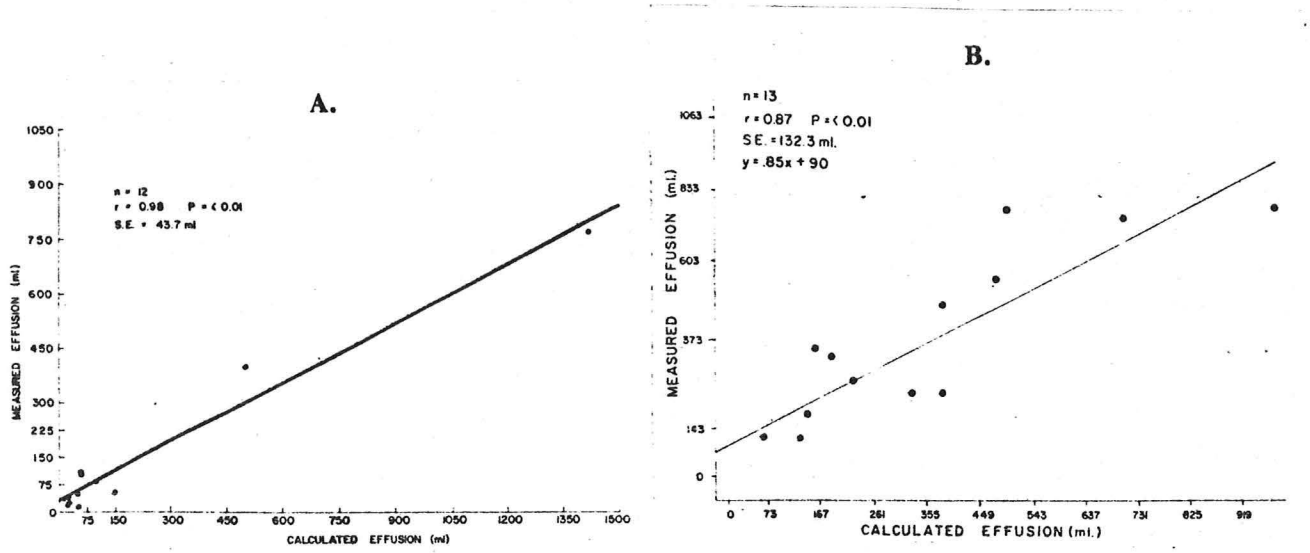

Figure 26: A shows plots of surgically measured pericardial effusions versus echocardiographically estimated effusions. B shows plots of effusions removed by pericardiocentesis versus echocardiographically estimated effusions (59).

The authors were well aware that the high correlation was a statistical quirk brought about by the reasonably accurate estimation of two large volumes. Despite the high correlation coefficient, the standard error of estimate remained large at 44 mls. They also compared the ultrasonic estimations of 13 patients undergoing paracentesis (Figure 26B). A more moderate linear correlation and much higher standard error of estimate of 132 mls were found.

A more recent study by Vignola and associates, attempted to correlate the amplitude and velocity of right and left ventricular free wall motion with the size of the pericardial effusion (60). From their paper, I have plotted their echocardiographic estimations according to their description of the size of the effusion in 28 echocardiograms obtained from 20 patients in Figure 27. Although they comment that posterior left ventricular wall diastolic velocity was significantly increased in the moderate and large effusions combined when compared to those with small effusions, the obvious overlap of all measurements would make any individual patient evaluation extremely difficult.

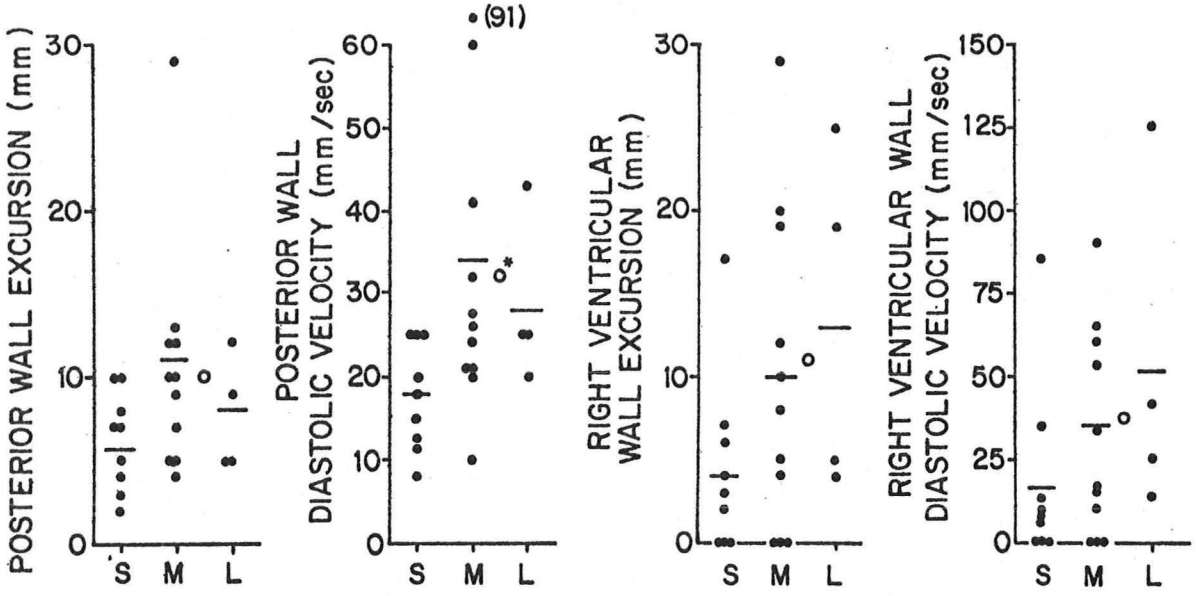

Figure 27: Plots of echocardiographic estimates of posterior left ventricular wall excursion and diastolic velocity, and anterior right ventricular wall excursion and diastolic velocity in 28 echocardiograms obtained from 20 patients with small (S), medium (M) or large (L) pericardial effusions.

*Significant difference between values for small versus medium and large effusions (from reference 60).

Although the presence of a pericardial effusion can be accurately identified, it is fair to say that its volume identified by echocardiogram can only be approximately estimated by currently available methods.

Comment should be made on the place of echocardiography in the diagnosis of cardiac tamponade. Early studies reported that the amplitude and velocity of the posterior left ventricular wall was diminished in these patients (58). Subsequently, it was reported that increased cardiac motion was associated with electrical and pulsus alternans (61,62). Recently, D'Cruz and associates have confirmed earlier direct hemodynamic studies of patients with cardiac tamponade. Figure 28 shows how, during inspiration, the right

ventricular dimension increases, the left ventricular dimension decreases and the mitral valve closing velocity (E to F slope) is reduced. Figure 29 illustrates these changes on a typical echocardiogram (65).

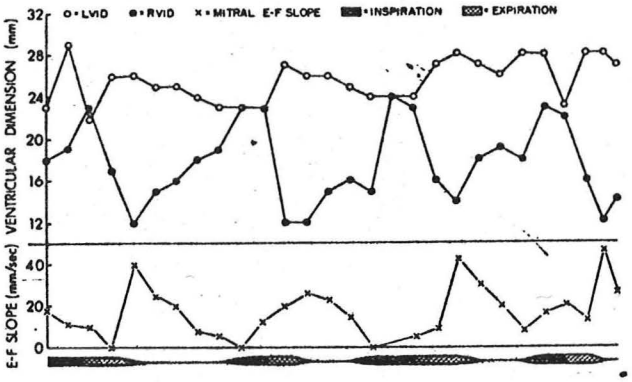

Figure 28: Serial plots of left ventricular end-diastolic diameter (LVID), right ventricular end-diastolic diameter (RVID), and mitral valve velocity (E-F slope) from a continuous echocardiogram in a patient with cardiac tamponade, showing how the diameters change during respiration (64).

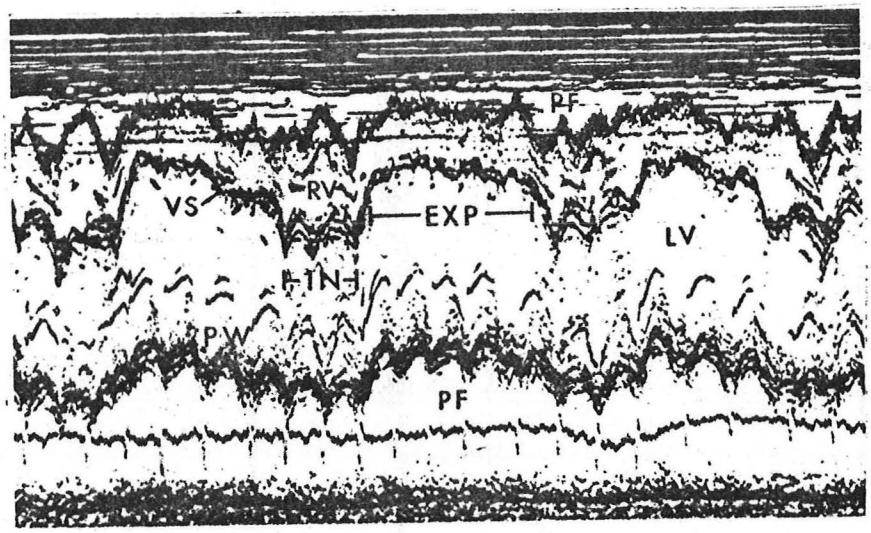

Figure 29: A typical echocardiogram of a patient with cardiac tamponade showing pronounced variations in cardiac dimensions during respiration. IN=inspiration; EXP=expiration; RV=right ventricle; VS=interventricular septum; LV=left ventricle; PW=posterior left ventricular wall; PF=pericardial fluid (65).

58. Feigenbaum, Waldhausen JA, Hyde LP: Ultrasonic diagnosis of pericardial effusion, JAMA 191:107, 1965.

59. Horowitz MS, Schultz CS, Stinson EB, Harrison DC, Popp RL: Sensitivity and specificity of echocardiographic diagnosis of pericardial effusion. Circulation 50:239, 1974.

60. Vignola PA, Pohost GM, Curfman GD, Myers GS: Correlation of echocardiographic and clinical findings in patients with pericardial effusion. Am J Cardiol 37:701, 1976.

61. Gabor GE, Winsberg F, Bloom HS: Electrical and mechanical alteration in pericardial effusion. Chest 59:341, 1971.

62. Usher BW, Popp RL: Electrical alternans: mechanism in pericardial effusion. Am Heart J 83:459, 1972.

63. Shabetai R, Fowler NO, Fenton JC, Masankay M: Pulsus paradoxus. J Clin Invest 44:1882, 1965.

64. D'Cruz IA, Cohen HC, Prabhv R, Glick G: Diagnosis of cardiac tamponade by echocardiography. Changes in mitral valve motion and ventricular dimensions, with special reference to paradoxical pulse. Circulation 52:460, 1965.

65. Tajik AJ: Echocardiography in pericardial effusion. Am J Med 63:29, 1977.

ENDOCARDITIS

The echocardiographic manifestations of valvular endocarditis include the demonstration of vegetations and flail and prolapsing valve leaflets (66,67). Associated hemodynamic abnormalities, particularly with aortic valve endocarditis, may also be seen on the echocardiogram (68-71). The issue as to what size a vegetation must be before it is detected during an ultrasonic examination has not yet been resolved (72). Dillon et.al. in their original report of the demonstration of vegetations stated that the echocardiogram detected vegetations of 2 to 8 mm in diameter when compared to surgical or autopsy measurements (66). More recently, studies on aortic valve endocarditis failed to demonstrate vegetations less than 5 mm in diameter (73). Real-time, two-dimensional techniques have also been used to identify vegetations. In a small series of seven patients, two-dimensional studies failed to detect vegetations of less than 2 mm in diameter (74). Figure 30 illustrates the growth of vegetations on the aortic valve of a patient from Parkland Memorial Hospital.

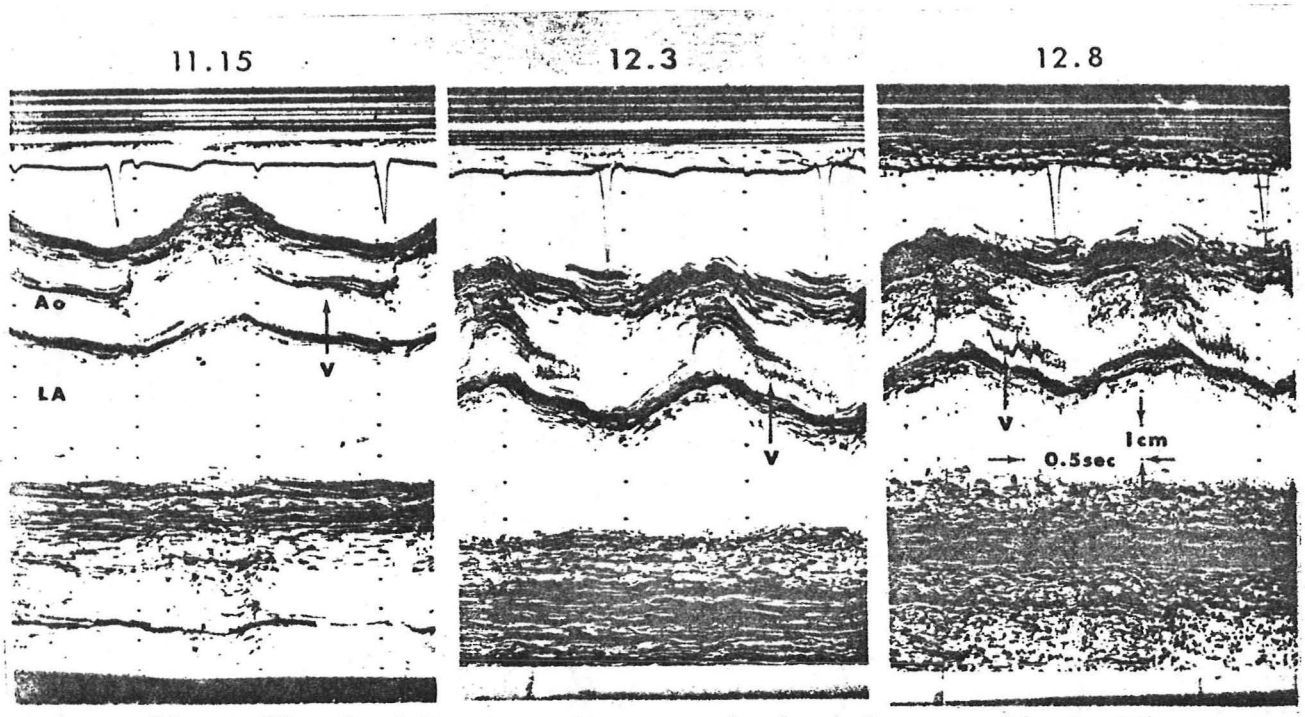

Figure 30: Serial echocardiograms obtained from a patient with acute aortic regurgitation due to endocarditis. V=vegetations; Ao=aortic root; LA=left atrium. Numbers refer to the month and day the studies were performed.

Irrespective of whether the minimal size for the ultrasonic detection of vegetations is 2 or 5 mm, it can be seen from this example that the admission study is non-specific. Thus, endocarditis must be established for a finite length of time before the echocardiogram is capable of demonstrating valvular vegetations.

A recent study reported 20 or 22 patients found to have vegetations on echocardiogram either died or underwent cardiac surgery, and concluded that this was a significant indication for early surgical intervention (75). These findings do not concur with those of Roy et.al. who studied 3 patients up to 18 months and continued to demonstrate vegetations by echocardiography after apparent clinical and bacteriological cure (67).

The hemodynamic derangements produced by acute aortic regurgitation due to endocarditis may be detected by echocardiogram (68-71, 76). The premature mitral valve closure, demonstrated in Figure 31, is due to the

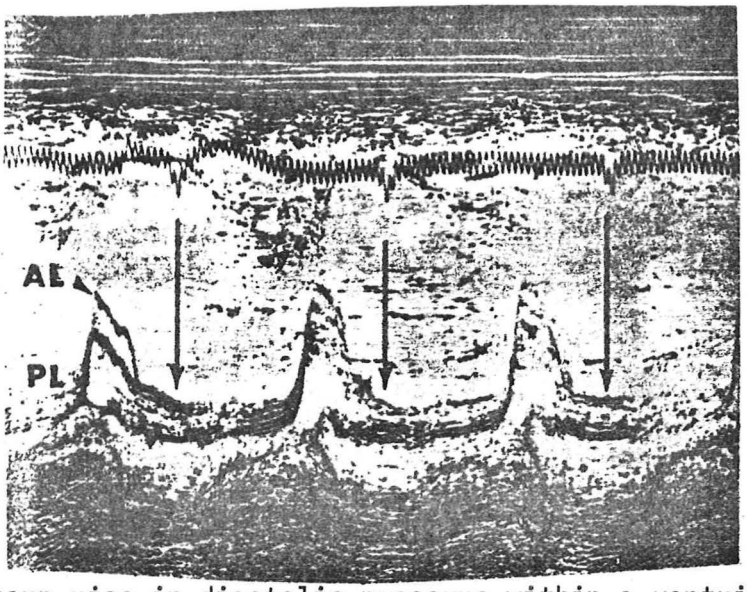

Figure 31: Premature mitral valve closure on an echocardiogram obtained from a patient with acute aortic regurgitation. The arrows indicate the normal point of mitral valve closure. AL= anterior leaflet; PL=posterior leaflet.

sharp rise in diastolic pressure within a ventricle unaccustomed to a volume overload. Because dilatation and eccentric hypertrophy, the primary compensatory mechanisms of the left ventricle, have insufficient time to develop in the acute situation, the result is a rise in diastolic pressure to levels greater than the left atrial pressure and premature closure of the mitral valve (Figure 32) (69).

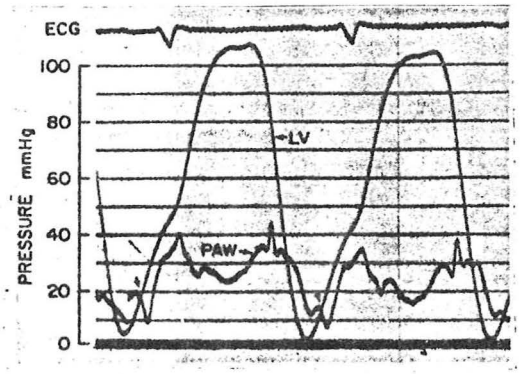

Figure 32: Simultaneous recording of the left ventricular (LV) and pulmonary capillary wedge (PAW) pressures in a patient with acute aortic regurgitation. The arrows indicate the premature intersection of the two pressure tracings which coincide with mitral valve closure (69).

In the absence of other defects, the degree of early valve closure correlated with the degree of elevation of the left ventricular end-diastolic pressure (69). Clearly, the demonstration of this echocardiographic finding is an indication for aortic valve replacement.

Thus, the echocardiogram is of particular value in the patient with endocarditis who develops acute valvular regurgitation. There is no doubt that ultrasonic studies are capable of identifying valvular vegetations, but the importance of demonstrating these findings with respect to the overall management of the patient with an established diagnosis of endocarditis remains unclear.

66. Dillon JC, Feigenbaum H, Konecke LL, Davis RH, Chang S: Echocardiographic manifestations of valvular vegetations. Am Heart J 86:698, 1973.

67. Roy P. Tajik AJ, Giuliani ER, Schattenburg TT, Gau GT, Grye RL: Spectrum of echocardiographic findings in bacterial endocarditis. Circulation 53:474, 1976.

68. Wise JR, Benton HH, Cleland WP, Goodwin JF, Halladie-Smith KA, Oakley CM: Urgent aortic-valve replacement for acute aortic regurgitation due to infective endocarditis. Lancet 2:115, 1971.

69. Mann T, McLaurin L, Grossman W, Craig E: Assessing the hemodynamic severity of acute aortic regurgitation due to infective endocarditis. N Engl J Med 293:108, 1975.

70. Botnevik EH, Schiller NB, Wickramasekaran R, Klauser SC, Gertz E: Echocardiographic demonstration of early mitral valve closure in severe aortic insufficiency: its clinical implications. Circulation 51:836, 1975.

71. DeMaria AN, King JF, Salel AF, Caudill CC, Miller RR, Mason DT: Echography and phonography of acute aortic regurgitation in bacterial endocarditis. Ann Intern Med 82:329, 1975.

72. Dillon JC: Echocardiography in valvular vegetations. Am J Med 62: 856, 1977.

73. Hirschfield DS, Schiller NB: Localization of aortic valve vegetations by echocardiography. Circulation 53:280, 1976.

74. Gilbert BW, Haney RS, Crawford F, McClellan J, Gallis HA, Johnson ML, Kisslo JA: Two-dimensional echocardiographic assessment of vegetative endocarditis. Circulation 55:346, 1977.

75. Wann WS, Dillon JC, Weyman AE, Feigenbaum H: Echocardiography in bacterial endocarditis. N Engl J Med 295:135, 1976.

76. Pridie RB, Benham R, Oakley CM: Echocardiography of the mitral valve in aortic valve disease. Br Heart J 33:296, 1971.

CONCLUSIONS

These are some examples of the value of ultrasound in the quantitative assessment of cardiac dysfunction. It is clear that in some disease states, echocardiography is capable of providing an accurate assessment of the severity of the disease. In certain cases, it is the procedure of choice. Nevertheless, much work still has to be done in this field to both improve the technique and expand its application.

Real-time, two-dimensional ultrasound represents a fascinating development that is already suggesting that the trend in diagnostic techniques in clinical cardiology is more and more towards noninvasive methods. Its

ability to visualize the whole heart in motion, together with its capability to accurately display normal or abnormal valvular orifices and ventricular outflow tract obstructions, and the presence or absence of significant atherosclerotic lesions in the left and right main coronary arteries, demonstrates that these techniques show great promise and suggests that their value and use can only increase in the near future.

Finally, the relatively easy adaptation of echocardiography to computer techniques has permitted not only the rapid online analysis of conventional tracings, but also the consideration of three-dimensional imaging and cardiac tissue characterization (77-79).

77. Saffer SI, Nixon JV, Mishelevich DJ: A simple method of computer-aided analysis of echocardiograms. Am J Cardiol 38:34, 1976.

78. Brinkley JF, Moritz WE, Baker DW: A technique for imaging three-dimensional structures and computing their volumes using non-parallel ultrasonic sector scans. Reflections 3:210, 1977.

79. Mimbs JW, Yuhas DE, Miller JG, Weiss AN, Sobel BE: Detection of myocardial infarction in vitro based on altered attenuation by ultrasound. Circ Res 41:192, 1977.